Biochimica et Biophysica Acta, 936 (1988) 171–178
Elsevier

BBA 42854

Polarographic studies of photocatalytic chlorophyll. Formation of chlorophyll *a* dihydrate dimer and oligomer in water-acetone binary solvent mixtures.

A. Agostiano [a], M. Caselli [a], M. Della Monica [a], A.J. Gotch [b] and F.K. Fong [b]

[a] *Department of Chemistry, Bari University, Bari (Italy) and* [b] *Department of Chemistry, Purdue University, West Lafayette, IN (U.S.A.)*

(Received 28 July 1988)

Key words: Photosynthesis; Chlorophyll *a* dihydrate; Water splitting; Polarography; Photoelectrochemistry

Polarographic techniques are employed in the investigation of Chl *a* dihydrate formation and aggregation in binary solvent mixtures of water/acetone. The variation of the relative intensities of two observed polarographic peaks, at ≈ -1100 and -1200 mV, with the composition of the binary solvent supports a shift in the equilibrium in favor of the formation of chlorophyll *a* dihydrate, Chl *a* · $2H_2O$, from the acetone solvate, Chl *a* · Ac, as the water concentration is increased. It is concluded that the equilibrium further shifts towards the dimerization of Chl *a* · $2H_2O$ at water concentrations exceeding 40% (volume). A third polarographic peak at -1434 mV, observed in 50:50 (v/v) water/acetone solutions at Chl *a* concentrations greater than $1 \cdot 10^{-5}$ M, is attributed to the oligomer of Chl *a* dihydrate, (Chl *a* · $2H_2O)_n$. From the amount of electricity calculated from the polarographic peaks, the coverage areas, 259 and 597 Å^2, are respectively obtained for the adsorbed monomer, Chl *a* · Ac, and dimer, (Chl *a* · $2H_2O)_2$, at the electrode surface.

Introduction

The in vitro oxidation and reduction reactions of water photocatalysed by the chlorophyll are of great current interest. Several research groups have reported the photo-oxidation of water by chlorophyll stabilized on a metal surface [1,2], on a bilayer lipid membrane [3,4], on aerosil [5], and at the interface between two immiscible liquids [6–8]. Chl *a* multilayers on Pt photocatalyses the splitting of deoxygenated water, leading to the simultaneous evolution of hydrogen and oxygen [9]. In the presence of CO_2, the hydrogen thus produced from water splitting reduces the carbon dioxide in photosynthesis in vitro of polyatomic organic molecules [10]. In oxygen-saturated water-acetone solutions, the illumination of the chlorophyll results in the formation of the superoxide radical anion, $O_2^{-\cdot}$ or its protonated form $HO_2^{\cdot}$ [11].

An important focus in this research is the characterization of the photocatalytic chlorophyll. The action spectra of the chlorophyll water photooxidation reaction using Chl *a* on a metal surface and at the interface of water and octane were found to follow closely [12,13] the absorption spectra of oligomeric hydrated chlorophyll [14,15] given by the dihydrate stoichiometry, (Chl *a* · $2H_2O)_n$. The catalytic cycles of the photoreactive chlorophyll were examined in the investigation of the electron spin resonance (ESR) lifetimes of the

Abbreviations: Chl, chlorophyll; PS II, Photosystem II.

Correspondence: F.K. Fong, Department of Chemistry, Purdue University, West Lafayette, IN 47907, U.S.A.

dimeric and oligomeric radical cations, (Chl $a \cdot 2H_2O)_2^{+\cdot}$ and (Chl $a \cdot 2H_2O)_n^{+\cdot}$, obtained upon illumination of water-saturated nonpolar solutions of Chl *a* [16]. The relaxation dynamics of photoexcited (Chl $a \cdot 2H_2O)_n$ in water-saturated nonpolar solutions was recently characterized by picosecond absorption [17] and fluorescence [18] measurements. The decay kinetics of the triplet state of hydrated Chl *a* ware determined by fluorometric techniques [19]. The role of singlet–triplet annihilation in upconverting the photoexcitation energy in (Chl $a \cdot 2H_2O)_n$ was examined by double optical-resonance techniques [20].

Current work [11,21] on hydrated Chl *a* aggregation and photochemistry has turned to Chl *a* solutions in water/acetone mixtures. Although the dramatic variations in the absorption and fluorescence properties of Chl *a* with the composition of the binary solvent mixtures were described by early workers nearly two decades ago [22,23], it was not until recently that attempts were made to relate the spectroscopic observations to Chl *a* aggregation as a consequence of its hydration behavior [21]. We recently made a quantitative correlation of the observed Chl *a* fluorescence quenching to the stoichiometric relationship between Chl *a* solvation by the acetone, Chl $a \cdot$ Ac, and Chl *a* hydration. It was shown [21] that the dihydrate dimer, (Chl $a \cdot 2H_2O)_2$, exists in comparatively small quantities in the presence of predominantly monomeric Chl *a* in the bulk solution up to 40 : 60 (v/v) in water/acetone composition. This equilibrium is given by:

$$2\text{Chl } a \cdot \text{Ac}(662\text{ nm}) + 4H_2O \rightleftharpoons (\text{Chl } a \cdot 2H_2O)_2(678\text{ nm}) + 2\text{Ac} \quad (1)$$

In reaction 1, the 662 nm absorbing Chl $a \cdot$ Ac monomer reacts with a stoichiometric amount of water to give the dihydrate dimer, which has a difference absorbance maximum at 678 nm [21]. At $5 \cdot 10^{-5}$ M Chl *a* concentration and water concentrations exceeding 40%, (Chl $a \cdot 2H_2O)_2$ was found to oligomerize, leading eventually to the precipitation of polycrystalline Chl *a* with the stoichiometry (Chl $a \cdot 2H_2O)_n$ [14]. The 678 nm absorbing Chl *a* dihydrate dimer has been previously proposed [1] as a model for P680, the reaction-center dimer [24] of PSII in green-plant photosynthesis.

In this paper, we wish to describe independent experimental methods and measurements for delineating the equilibrating Chl *a* species in reaction 1. A particularly suitable method is polarography, althcugh its applicability to the study of Chl *a* aggregation and related problems has not been widely realized.

In solutions of a strongly adsorbed electrolyte, the adsorption process is controlled by transport towards the electrode [25]. The hanging mercury drop is maintained at a fixed potential for a given time in order to accumulate the adsorbed molecules at the electrode. The accumulation process depends on the bulk concentration and the potential at which the electrode is maintained. As the potential is varied, two different processes can possibly take place simultaneously at the electrode [26,27]. First, the adsorbed molecules at the electrode surface could undergo desorption, changing the capacity of the electrode, thus causing a capacitative current to flow in the external circuit. Second, the adsorbed molecules could undergo electrochemical reaction, and a corresponding Faradaic current is recorded. In the case of physical desorption, it is possible to record a tensammetric curve that presents a step maximum corresponding to the desorption. Generally this process occurs when the surface becomes sufficiently negative [26].

In applying the above considerations to a study of reaction 1, the intensities of any observed polarographic peaks would be expected to be dependent upon the kinetic processes relating the Chl *a*-solvent complexes/aggregates in the solution and the adsorbed Chl *a* at the electrode surface. It should be possible to differentiate the polarographic behavior of the equilibrating Chl *a* aggregates, and correlate this behavior with the observed spectroscopic changes that attend the same equilibrating processes. The purpose of this paper is to demonstrate a corroboration of the spectroscopic determination [21] of reaction 1 using polarographic techniques.

Experimental procedures

Chl *a* was extracted from spinach and purified, and stock solutions of the purified chlorophyll

were prepared according to the methods reported by Brace et al. [14]. Appropriate amounts of freshly prepared stock solution were evaporated to dryness. Acetone was added to dissolve the chlorophyll. The required amount of water was then slowly added to make 0:100–50:50 (v/v) water/acetone solutions. The absorption spectra of the Chl *a* solutions thus prepared were recorded using a Perkin-Elmer Model 555. The sample turbidity was monitored by light-scattering experiments using He/Ne laser (Coherent Research Model CR-80) excitation at 632.8 nm, in which the scattered light at right angle to the incident laser source was detected using a photomultiplier tube (RCA 7265).

Two different methods of potential scan were used in the voltammetric measurements. The first method used a triangular sweep, in which the potential was linearly changed up to a fixed value and then returned to the initial value with the same or different potential sweep rates. In the second method, a differential pulse was employed, in which the potential was varied linearly, at a rate of a few mV/s, superimposed by a 50 ms square pulse of 25 or 50 mV. The difference between the current sampled during the last 17 ms of the pulse and that measured before the pulse was recorded [28].

A PAR 174A polarograph, connected with an E.G.&G. xy recorder (Model RE0089), was used for the differential pulse measurements. Fast triangular sweeps were carried out using a function generator (Amel 566) and a storage oscilloscope (Gould OS 4000). A hanging mercury drop electrode (Metrohm EA 290/1) was used as the working electrode. The drop surface was 1.39 mm^2. In the differential pulse measurements, a scan rate of 10 mV/s was employed. For fast triangular sweep, measurements were performed at sweep rates of 5, 10 and 20 V/s. The sample temperature was maintained at 25 ± 0.2°C.

Experimental results

The laser light-scattering experiments indicate that the turbidity due to Chl *a* in freshly prepared solutions is approximately the same from 0:100 to 50:50 in water/acetone compositions. At water concentrations exceeding 50%, a dramatic increase in the scattered light intensity due to colloid formation of the chlorophyll was observed. All measurements reported in the following relate to binary solvent mixtures up to 50% in water concentrations.

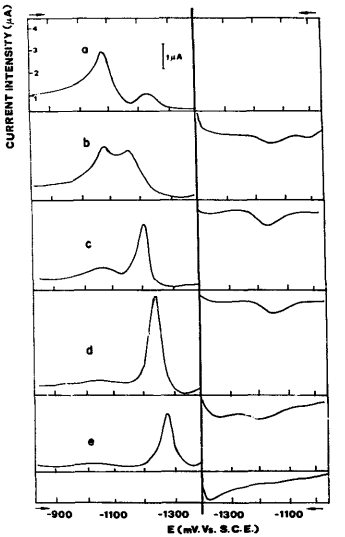

Fig. 1. Triangular voltammograms of $1 \cdot 10^{-6}$ M Chl *a* solutions in (a) 10:90, (b) 20:80, (c) 30:70, (d) 40:60, and (e) 50:50 water/acetone mixtures. Supporting electrolyte: 0.1 M $NaClO_4$. Scan rate = 5 V/s. Accumulation potential = −200 mV. Accumulation time = 1 min. All potentials are vs. S.C.E.

The observed currents from a mercury drop upon application of a fast triangular potential sweep are shown for $1.0 \cdot 10^{-6}$ M Chl *a* solutions in 10:90, 20:80, 30:70, 40:60 and 50:50 water/acetone mixtures (figs. 1a–e).

Two well-defined peaks at ≈ −1100 and ≈ −1200 mV (S.C.E.), shown in Fig. 1a, were recorded after a −200 mV potential was maintained for 1 min. In Fig. 1a, the current peak at ≈ −1100 mV is significantly greater than that at ≈ −1200 mV. An increase in the water content of the Chl *a*

TABLE I

POTENTIAL MAXIMA OF PEAKS I AND II

Potential maxima of peak I and II for five compositions (v/v) of water/acetone measured at three different scan rates ($a = 5$ V/s, $b = 10$ V/s and $c = 20$ V/s). All potentials are measured vs. S.C.E.

Composition (v/v)	Potential maxima (mV)					
	a		b		c	
	I	II	I	II	I	II
10:90	-1,084	-1,200	-1,110	-1,257	-1,110	-1,257
20:80	-1,110	-1,187	-1,142	-1,226	-1,163	-1,252
30:70	-1,114	-1,237	-	-1,260	-	-2,280
40:60	-	-1,289	-	-1,296	-	-1,306
50:50	-	-1,326	-	-1,339	-	-1,356

solution is accompanied by an increase in intensity of the peak at the more negative potential (peak II) relative to that at the less negative potential (peak I), as evidenced by the progression shown in Figs. 1a–e. An increase of the water content to 40 and 50% in volume results in the virtual disappearance of the first peak. A single peak at −1270 mV predominates the voltammogram for the 50:50 water/acetone solution. In all runs, a broad, less well-defined band is observed on the reverse scan (Figs. 1a–e).

A dependence of the peak potential on the solvent composition is also noted. The potentials for the current maxima at different solvent

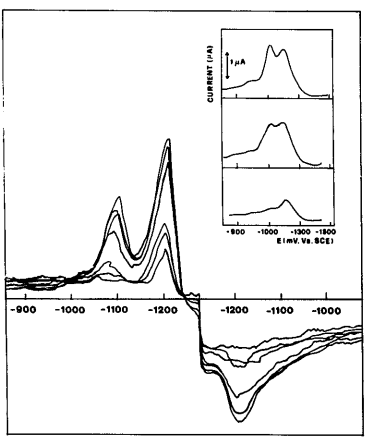

Fig. 2. Successive scans at the same drop for $1 \cdot 10^{-6}$ M Chl *a* in 20:80 water/acetone. All experimental conditions are the same as those in Fig. 1. Inset: voltammograms from successive potential scans of a $0.2 \cdot 10^{-6}$ M Chl *a* solution in 20:80 water/acetone. Bottom to top: 1, 2 and 3 min of accumulation at −200 mV.

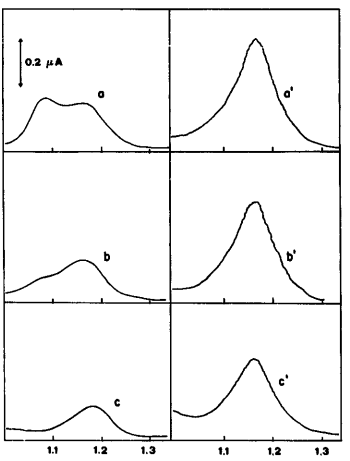

Fig. 3. Differential pulse measurements of $2.0 \cdot 10^{-7}$ M Chl *a* in 20:80 water/acetone (a–c) and 40:60 water/acetone (a′–c′) after (a, a′) 1, (b, b′) 2 and (c, c′) 3 min of accumulation at -200 mV. Scan rate = 10 mV/s.

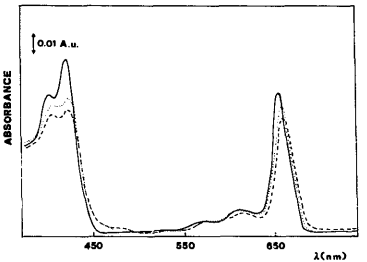

Fig. 4. Absorption spectra of $1 \cdot 10^{-6}$ M Chl *a* in acetone (———), 30:70 water/acetone (·····) and 50:50 water-acetone (- - - - -).

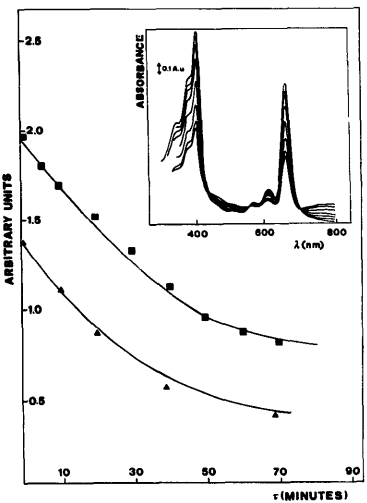

Fig. 5. Absorbance (■) and current intensity of peak II (▲) plotted against time for $5 \cdot 10^{-5}$ M Chl *a* in 50:50 water/acetone. Inset: absorbance spectral changes with time for a $5 \cdot 10^{-5}$ M Chl *a* solution in 50:50 water/acetone.

compositions, for three different scan rates, are summarized in Table I.

The intensities of the two voltammetric peaks decrease simultaneously upon successive potential scans at the same mercury drop (Fig. 2). A dramatic dependence of the relative intensities of the two peaks on the accumulation time is demonstrated for a $2.0 \cdot 10^{-7}$ M Chl *a* solution in 20:80 water/acetone (see, inset, Fig. 2).

The above-described results obtained using the fast triangular sweep method are entirely confirmed by the differential pulse measurements, as shown in Fig. 3 for $2.0 \cdot 10^{-7}$ M Chl *a* solutions in 20:80 and 40:60 water/acetone mixtures after 1, 2 and 3 min accumulation with the electrode maintained at −200 mV. The presence of two polarographic peaks having different dependence on the accumulation time is found for the 20:80 water/acetone solution. As in the case reported above using a triangular sweep (Fig. 1), an increase in the water content to 40% results in the virtual disappearance of peak I.

The absorption spectra of $1 \cdot 10^{-6}$ M Chl *a* solutions in pure acetone and in 30:70 and 50:50 water/acetone mixtures, recorded under the same conditions as those under which the results shown in Fig. 1 were measured, are reproduced in Fig. 4.

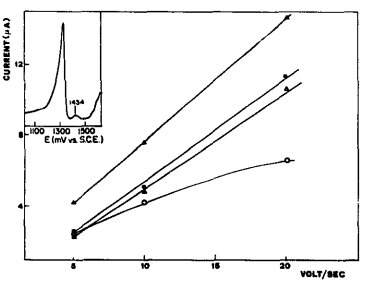

Fig. 6. Current intensity of peak II plotted against scan rate for $1 \cdot 10^{-6}$ M Chl *a* solutions in 20:80 (△), 30:70 (■), 40:60 (▲), and 50:50 (○) water-acetone mixtures. Accumulation time = 1 min. Accumulation potential = −200 mV. Inset: Polarographic measurement of a $1 \cdot 10^{-5}$ M Chl *a* solution in 50:50 water/acetone. Accumulation time = 3 min. Accumulation potential = −200 mV.

Changes in the wavelength positions and intensities of the absorption bands as a function of increasing water concentrations are shown. A FWHM increase for the red absorption band of the Chl *a* in 50:50 water/acetone from that in pure acetone is observed. Increasing the Chl *a* concentration up to $5 \cdot 10^{-5}$ M, in 40:60 and 50:50 water/acetone mixtures, triggers the precipitation of polycrystalline $(\text{Chl } a \cdot 2H_2O)_n$ [14,15,29], which, of course, is manifested by a corresponding decrease in the absorbance of the Chl *a* solution. The decay in the absorption intensity is accompanied by the growth of a long-wavelength absorption component due to oligomerization of the hydrated Chl *a* [12–15,29]. The temporal changes in the absorption spectrum of a $5 \cdot 10^{-5}$ M Chl *a* solution in 50:50 water/acetone are illustrated in the inset of Fig. 5. Note the intensity of the red absorption band of a $5 \cdot 10^{-5}$ M Chl *a* solution in 50:50 water/acetone decays concurrently with that of peak II. Also, the appearance of the long-wavelength absorption band (inset, Fig. 5) is accompanied by the appearance of a new peak at −1434 mV (inset, Fig. 6). No evidence of this peak was found for Chl *a* concentrations lower than $1 \cdot 10^{-5}$ M.

Discussion

The observed polarographic peaks could conceivably be due to a combination of Faradaic and tensammetric currents arising, respectively, from electrochemical reaction and physical desorption [30]. However, the closeness in value of the peak potentials with the reduction potential of Chl *a* [31] is suggestive of an electrochemical, irreversible reduction of two distinct adsorbed Chl *a* species, in which the reaction products are also adsorbed on the drop surface [32]. This hypothesis is supported by the presence of the small reoxidation peak on the reverse scan and by the value of the peak width (≈ 90 mV) in the differential pulse polarographic measurements.

The different dependence on the accumulation time of peaks I and II (see, inset, Fig. 2 and Fig. 3) is indicative of the presence of at least two Chl *a* solvation complexes with distinctly different adsorption/desorption kinetics. The progressive disappearance of peak I with increasing water content suggests a progressive shift of the solvation equilibrium from Chl $a \cdot$ Ac towards the formation of the hydration complex, Chl $a \cdot 2H_2O$:

$$\text{Chl } a \cdot \text{Ac} + 2H_2O \rightleftharpoons \text{Chl } a \cdot 2H_2O + \text{Ac} \qquad (2)$$

At a water content greater than 30%, peak I has virtually vanished, which suggests that the Chl *a* exists mostly as the dihydrate.

A linear dependence of the current intensities of peak II on the scan speed for Chl *a* in 20:80, 30:70 and 40:60 water/acetone is observed (Fig. 6). This linear dependence clearly indicates that the kinetic process is controlled by an adsorption mechanism involving predominantly a single species, the Chl *a* dihydrate monomer according to reaction 2. The deviation from linearity observed in Fig. 6 for Chl *a* in 50:50 water/acetone can be ascribed to a further shift of the Chl *a* equilibrium towards dimerization of the dihydrate:

$$2\text{Chl } a \cdot 2H_2O \rightleftharpoons (\text{Chl } a \cdot 2H_2O)_2 \qquad (3)$$

which controls the adsorption/desorption kinetics. The increase in the FWHM of the red absorption band of the Chl *a* in 50:50 water/acetone (Fig. 4) is due to the appearance of the 678 nm band of the $(\text{Chl } a \cdot 2H_2O)_2$ [21]. This conclusion is corroborated by the data shown in Fig. 7, in which the current intensities of peak II are plotted against the water content for three different scan rates. The current intensity increases with increasing water content up to 40% water. The subsequent decrease in the current intensity as the water content increases to 50% thus supports the formation of a new Chl *a* aggregate, consistent with the dimerization conclusion given by reaction 3. The polarographic peak at −1434 mV observed in 50:50 water/acetone solutions at Chl *a* concentrations greater than $1 \cdot 10^{-5}$ M (inset, Fig. 6) is accordingly attributed to the hydrated Chl *a* oligomer, $(\text{Chl } a \cdot 2H_2O)_n$, whose appearance is also noted as the long-wavelength component in the absorption spectra shown in the inset of Fig. 5.

The above-described results and interpretations are in complete agreement with the conclusions drawn from spectroscopic measurements [21]. In this earlier investigation, it was reported that the concentration of $(\text{Chl } a \cdot 2H_2O)_2$, denoted by C_A

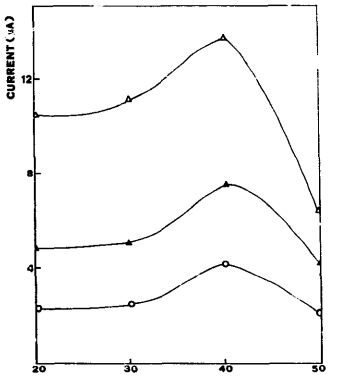

Fig. 7. Current intensity of peak II plotted against water content in volume % for $1 \cdot 10^{-6}$ M Chl *a* in water-acetone. Scan rate: (○) 5 V/s, (▲) 10 V/s, and (△) 20 V/s. Accumulation time = 1 min. Accumulation potential = −200 mV/s.

as the concentration of the energy acceptor or fluorescence quencher, is small relative to that of the bulk (monomeric) Chl *a* up to 40% water. The earlier work further concluded that, at water concentrations greater than 40%, extensive dimerization of the Chl *a* dihydrate results in the formation of hydrated Chl *a* oligomer in a $5 \cdot 10^{-5}$ M solution in 50:50 water/acetone, leading to the precipitation of polycrystalline $(\text{Chl } a \cdot 2H_2O)_n$. The Chl *a* dihydrate stoichiometry assignment for this polycrystalline chlorophyll has been based on X-ray photoelectron spectroscopic [14] and thermogravimetric [15] determinations. This assignment corroborates that given by an X-ray diffraction study of single crystalline ethyl chlorophyllide dihydrate [33].

The spectral distributions and lifetimes of Chl $a \cdot$ Ac and Chl $a \cdot 2H_2O$ were not resolvable in the absorption and fluorescence spectroscopic measurements [21–23]. The present study provides a detailed characterization of the Chl *a* equilibrating processes in reactions 2 and 3, the sum of which, of course, yields reaction 1, as concluded in the fluorescence quenching study [21]. In reaction 2 the equilibrating Chl *a* acetone solvate and hydrate, Chl $a \cdot$ Ac and Chl $a \cdot 2H_2O$, have been identified as separate entities on the grounds of differentiable kinetic processes in polarographic measurements.

From the amount of electricity calculated from peaks I and II (Fig. 1), assuming a one-electron process [26], the value obtained for the drop coverage amounts to a monolayer of the Chl *a* adsorbed at the electrode surface, in the order of 10^{13} molecules cm^{-2}. The reciprocal of this value gives the coverage area per adsorbed Chl *a* complex. This area is found to be 259 $Å^2$ for Chl *a* in 20:20 water/acetone, which is in reasonable agreement with that, 270 $Å^2$, reported for a single adsorbed molecule of Chl *a* [34]. The corresponding area obtained for a 50:50 water/acetone solution of Chl *a* at the scan speed 20 V/s is 597 $Å^2$, which corroborates the conclusion that the adsorbed Chl *a* in this case occurs as the dihydrate dimer, $(\text{Chl } a \cdot 2H_2O)_2$.

The electrochemical method described above has thus proven to be a versatile tool for investigating the physicochemical properties of chlorophyll aggregation in the appropriate solvent media, providing corroboration and extending the scope of this investigation beyond that of the spectroscopic studies of in vitro Chl *a* models for photosynthesis. A polarographic study of the Chl a-H_2O aggregation process occurring at water concentrations greatly exceeding 50% in the binary mixtures will be described elsewhere.

Acknowledgments

We are grateful to Dr. E. Palecek for helpful discussions on the calculation of the coverage areas at the electrode surface.

References

1 Fong, F.K. (1982) in Molecular Biology and Biophysics. Light Reaction Path of Photosynthesis (Fong, F.K., ed.), Vol. 35, part I, pp. 277–329, Springer Verlag, Heidelberg.
2 Fong, F.K. and Winograd, N. (1976) J. Am. Chem. Soc. 98, 2287–2290.
3 Toyoshima, Y., Marino, M., Motoki, H. and Sukigara, M. (1977) Nature 265, 187–189.
4 Sukigara, M. and Kurihara, K. (1980) in Third Interna-

tional Conference of Photochemical Conversion and Storage of Solar Energy (Connoly, J.S., ed.), August 3–8, 1980, pp. 77–79, Solar Energy Research Institute, University of Colorado, Boulder, CO.
5 Kachan, A.A. and Neghievich, L.A. (1978) Doklady Akad. Nauk SSSR 241, 1304–1206 (in Russian).
6 Volkov, A.G., Kolev, V.D., Levin, A.L. and Boguslavsky, L.I. (1985) Photobiochem. Photobiophys. 10, 105–111.
7 Volkov, A.G. (1986) J. Electroanal. Chem. 205, 245–257.
8 Kandelaki, M.D., Volkov, A.G., Shubin, V.V. and Boguslavsky, L.I. (1987) Biochim. Biophys. Acta 893, 170–76.
9 Fong, F.K. and Galloway, L. (1978) J. Am. Chem. Soc. 100, 3594–3597.
10 Fruge, D.R., Fong, G.D. and Fong, F.K. (1979) J. Am. Chem. Soc. 101, 3694–3698.
11 You, J.-L. and Fong, F.K. (1986) Biochem. Biophys. Res. Commun. 139, 1124–1129.
12 Showell, M.S. and Fong, F.K. (1982) J. Am. Chem. Soc. 104, 2773–2781.
13 Kandelaki, M.D., Volkov, A.G., Levin, A.L. and Boguslavsky, L.I. (1983) Bioelectrochem. Bioenerg. 10, 167–172.
14 Brace, J.G., Fong, F.K., Karweik, D.H., Koester, V.J., Shepard, A. and Winograd, N. (1978) J. Am. Chem. Soc. 100, 5203–5207.
15 Blaha, H., Kis, P. and Springer-Lederer, H. (1981) Anal. Biochem. 112, 282–286.
16 Fong, F.K., Kusunoki, M., Galloway, L., Matthews, T.G., Lytle, F.E., Hoff, A.J. and Brinkman, F.A. (1982) J. Am. Chem. Soc. 104, 2759–2767.
17 Maly, P., Danielius, R. and Gadonas, R. (1987) Photochem. Photobiol. 45, 7–11.
18 Alfano, A.J., Lytle, F.E., Showell, M.S. and Fong, F.K. (1985) J. Chem. Phys. 82, 758–764.
19 Alfano, A.J., Showell, M.s. and Fong, F.K. (1985) J. Chem. Phys. 82, 765–772.
20 Alfano, A.J. and Fong, F.K. (1982) J. Am. Chem. Soc. 104, 2768–2733.
21 Agostiano, A., Butcher, K.A., Showell, M.S., Gotch, A.J. and Fong, F.K. (1987) Chem. Phys. Lett. 137, 37–41.
22 Hochapfel, A., Journeaux, R. and Viovy, R. (1969) J. Chim. Phys. 66, 1467–1473.
23 Journeaux, R., Hochapfel, A. and Viovy, R. (1969) J. Chim. Phys. 66, 1474–1478.
24 Den Blanken, H.J. and Hoff, A.J., (1983) FEBS Lett. 157, 21–25.
25 Batina, N., Ruzic, I. and Cosovic, B. (1985) J. Electroanal. Chem. 190, 21–32.
26 Bard, A.J. and Faulkner, L.R. (1980) Electrochemical method, pp. 515–531, John Wiley&Sons, New York.
27 Brainina, K.Z. (1981) Bioelectrochem. Bioenerg. 8, 479–485.
28 Willard, H.H., Merrit, L.L., Dean, J.A. and Seattle, F.A. (1980) Instrumental methods of analysis, Chapter 24, Van Nostrand, New York.
29 Fong, F.K. and Koester, V.J. (1976) Biochim. Biophys. Acta 423, 52–64.
30 Palecek, E., Jelen, F. and Manousek, O. (1980) Coll. Czech. Chem. Commun. 45, 3460–3471.
31 Kiselev, B.A. and Kozlov, Y.N. (1980) Bioelectrochem. Bioenerg. 7. 247–254.
32 Krznaric, D., Valenta, P. and Nurnberg, H.W. (1975) J. Electroanal. Chem. 65, 863–881.
33 Chow, H.C., Serlin, R. and Strouse, C.E. (1975) J. Am. Chem. Soc. 97, 7230–7237.
34 Khanova, L.A. and Tarasevich, M.R., (1979) J. Electroanal. Chem. 104, 155–163.